Acta Crystallographica Section D
Biological Crystallography
ISSN 0907-4449

An ensemble of crystallographic models enables the description of novel bromate-oxoanion species trapped within a protein crystal

Jan Ondráček[a]* and Jeroen R. Mesters[b]

[a]Department of Recombinant Expression and Structural Biology, Institute of Molecular Genetics, Academy of Sciences of the Czech Republic, Flemingovo namesti 2, CZ-16637 Praha 6, Czech Republic, and [b]Institute of Biochemistry, Center for Structural and Cell Biology in Medicine, University of Lübeck, Ratzeburger Allee 160, D-23538 Lübeck, Germany

Correspondence e-mail: ondracek@img.cas.cz

Received 22 March 2006
Accepted 7 June 2006

PDB Reference: lysozyme containing bromate ions, 2d6b, r2d6bsf.

Only a few protein–oxoanion crystal complexes have been described to date. Here, the structure of a protein soaked in a bromate solution has been determined to a resolution of 1.25 Å and refined to final overall $R/R_{\rm free}$ values of 18.04/21.3 (isotropic) and 11.25/14.67 (anisotropic). In contrast to the single-model approach, refinement of an ensemble of ten models enabled us to determine variances and statistically evaluate bond-length distances and angles in the oxoanions. In total, nine bromate positions, including two $BrO_3^-\cdot HBrO_3$ dimer species, have been identified on the basis of the anomalous signal of the Br atoms. For all bromate ions, the main-chain amide atoms of the protein were identified as the dominant binding positions, a useful property in any experimental phase-determination experiment.

1. Introduction

In the presence of an anomalously scattering atom, the structure and absolute configuration of a small molecule can easily be determined to high resolution using X-ray crystallography. In the case that crystals cannot be obtained, the solution and solid-state structures mostly remain obscure. However, if the small molecule can be trapped inside a protein crystal, its absolute structure can again be determined, at least to medium resolution. Not only can the structure of an otherwise unknown (oxoanion) species be determined in this way, but also new or different species could be identified in contrast to those determined from inorganic crystal structures. An example of such an approach was published for periodate oxoanions trapped within a hen egg-white lysozyme crystal (Ondráček *et al.*, 2005). Four different periodate octahedron species, corresponding to $[I(OH)_4O_2]^{1-}$, $[I(OH)_5O]$, $[I(OH)_3O_3]^{2-}$ and $[I(OH)_6]^{1+}$, were found and, depending on the chemical environment, periodate seems to be able to accept or release H^+ and thereby balance its charge accordingly.

Protein–oxoanion complexes have rarely been studied (reviewed by Ondráček *et al.* (2005) and as a result nothing is known about the binding modes of various inorganic oxoanions. So far, protein-bound bromates have not been studied at all, let alone exploited for experimental phase determination. In this paper, we describe the structure and binding mode of bromate oxoanions trapped within a tetragonal hen egg-white lysozyme crystal. Normally, a deformed octahedral arrangement (three Br—O bonds and three Br···O contacts) is found in inorganic bromate-oxoanion crystals. Depending on both the space group and cation present, either sodium (space group $P2_13$; Abrahams & Bernstein, 1977; Templeton & Templeton, 1985) or potassium [space group $R3mr$ (Szafranski & Stahl, 1994); space group $R3mh$; Templeton &

Templeton, 1985], the Br—O distance can vary from 1.648 to 1.653 Å, the O—Br—O angle from 104.5 to 104.65° and the Br···O distance from 3.678 to 3.371 Å. Deviations in both distances and angles were observed for bromate species trapped within a protein crystal. The basic binding mode of these oxoanions substantiates their potential for the use in obtaining experimental phase information and as such they may offer a possible alternative to halide soaking (Dauter & Dauter, 1999, 2001; Dauter *et al.*, 2000, 2001).

2. Materials and methods

2.1. Crystal growth and soaking

Lysozyme crystals were grown employing the hanging-drop vapour-diffusion method: 2 µl each of protein stock solution (30 mg ml^{-1} hen egg-white lysozyme in 50 m*M* sodium acetate pH 4.8) and reservoir solution [6–10%(*w*/*v*) sodium chloride in 50 m*M* sodium acetate pH 4.8] were mixed. The soaking solutions were prepared as follows. PEG 400 was mixed with a 1 *M* solution of $NaBrO_3$ in a 1:1 ratio (solution I). Solution II was prepared by mixing reservoir and solution I in a 1:1 ratio. Solution III was prepared by mixing reservoir and solution II in a 1:1 ratio and so on. Finally, solution VI was obtained by mixing solutions I and II in a 1:1 ratio. The lysozyme crystals were gradually soaked for 2 min in solutions V, IV, III and II in turn and finally soaked for 10–15 min in solution VI. The crystals were immediately stored under liquid nitrogen.

2.2. Data collection and refinement

One high-resolution data set was collected at 100 K using synchrotron radiation (λ = 0.804 Å) at the EMBL beamline X13, Deutsches Elektronen-Synchrotron (Hamburg, Germany), equipped with a MAR CCD detector (X-ray Research, Hamburg). The Friedel pairs were not merged during data reduction (see Table 1).

The PDB entry 1hel (Wilson *et al.*, 1992) without solvent molecules was used as a starting model, applying the conjugate-gradient algorithm (CGLS) as implemented in the program *SHELX*97 (Sheldrick & Schneider, 1997). After placing the bromates and nearly all water molecules by hand, a full-matrix (least-squares) refinement using anomalous data was performed (Table 2, 'Input' column). Because of uncertainties in the construction of this model, we started to calculate an ensemble of structures (see below): each single model is equally compatible with the crystallographic data and the ensemble of models better describes the uncertainty of the experimental data and the structural microheterogeneity.

We generated a set of models using a water-building stage (both addition and removal) followed by a manual inspection and rebuilding stage. In detail, 150 maxima in the difference Fourier synthesis fulfilling a geometrical criterion (1.4 Å < distance from protein < 3.8 Å) were added as additional water molecules (U = 1.2, occupancy = 0.5) to the single structural model calculated above. During five subsequent cycles, water molecules not having (i) a ball-shaped electron density, (ii) a distance to protein atoms of less than than 1.1 Å and (iii) an electron-density level below 0.05, 0.15, 0.25, 0.35 and 0.45 e Å^{-3} in the first, second, third, fourth and fifth cycles, respectively, were gradually excluded. Every cycle was followed by 200 cycles of anomalous isotropic CGLS refinement. The resulting model (*i.e.* model 1) was then used to calculate a new model (*i.e.* model 2, repeating the procedure described above) and so on. After calculating ten structures, model 10 was manually improved utilizing details of the preceding nine structures. This model was then used to start a new cycle of calculations, leading to models 11–20. Model 20 was again manually improved using details of the preceding nine structures (*i.e.* models 11–19). Model 20 was then used for calculating the final set of ten structures (*i.e.* models 21–30). The labour-intense water-building stage has been automated and the software is available at http://www.img.cas.cz/hiphop.

Table 1
Data-collection statistics (Collaborative Computational Project, Number 4, 1994; Otwinowski & Minor, 1997).

Space group	$P4_32_12$
Unit-cell parameters (Å)	a = 77.210, c = 38.191
Wavelength (Å)	0.804
Crystal-to-detector distance (mm)	100
No. of images	180
Rotation per image (°)	0.5
Resolution range (Å)	50.0–1.25
Total No. of reflections	462667
No. of unique reflections	32334
Completeness overall (%)	99.4
$I/\sigma(I)$	27.9
$R_{\rm merge}$ (%)	5.6

Table 2 shows the anomalous refinement results of the ten final models and their mean averages ('Mean_ano' column). The anisotropic equivalents in Table 2 were calculated employing 1000 CGLS cycles: only atoms with an occupancy of 1 and all bromines were refined anisotropically (about 83% of all atoms in the models). The column called 'Mean_ave' represents an arithmetically averaged reflection value as calculated from the *SHELX* fcf output file (no anomalous contribution). A mean crystallographic vector structure factor calculated from all ten final structures is given in the 'Overall' column. In the multi-conformer PDB file (RCSB ID 025040, PDB code 2d6b), each single structure is labelled using a different MODEL number.

3. Results

3.1. Model building and refinement

During the first stages of manual model building, the following disordered residues were found: ND of Lys1, CG1, CG2 and CD1 of Ile55, OG of Ser86 and CG, CD, CE and NZ of Lys97. Additional disorder was modelled during subsequent refinement stages (see Fig. 1): for CG, OD1 and OD2 of Asp52 and CG of Pro79. Fig. 2 shows a compilation of the most disordered amino-acid side-chain residues (Arg21, Arg61, Arg73 and Arg128) after complete refinement.

The final reliability values of the set of models are an overall isotropic/anisotropic R factor of 18.04/11.25 and an overall

Table 2
Refinement statistics of the final ten models.

Model	Input	1	2	3	4	5	6	7	8	9	10	Mean_ano	Mean_ave	Overall
Isotropic refinement														
R	18.45	17.99	18.00	17.94	18.08	17.93	18.06	17.97	17.96	17.92	17.88	17.97 (6)	18.36 (6)	18.04
R (90% set)	18.20	17.81	17.84	17.75	17.95	17.78	17.94	17.80	17.84	17.75	17.71	17.82 (7)	18.20 (8)	17.81
R_{free} (10% set)	21.23	21.16	21.43	21.50	21.43	21.40	21.34	21.42	20.72	21.03	21.00	21.2 (2)	21.9 (3)	21.3
wR_2	49.32	48.18	48.17	48.16	48.33	48.07	48.32	48.20	48.21	48.19	48.13	48.20 (7)	—	—
S	2.639	2.570	2.569	2.569	2.580	2.564	2.579	2.571	2.571	2.570	2.566	2.571 (5)	—	—
No. of waters	213	298	303	302	293	307	292	291	292	290	295	296 (6)	—	—
Anisotropic refinement														
R	—	11.42	11.32	11.45	11.48	11.35	11.47	11.42	11.43	11.47	11.39	11.42 (5)	11.74 (5)	11.25
R (90% set)	—	11.15	11.04	11.17	11.21	11.08	11.16	11.22	11.23	11.25	11.09	11.16 (7)	11.47 (7)	10.96
R_{free} (10% set)	—	15.58	15.60	15.50	15.44	15.51	15.46	15.42	15.06	15.17	15.61	15.44 (17)	15.80 (20)	14.67
wR_2	—	29.07	29.02	29.20	29.25	29.02	29.28	29.26	29.32	29.44	29.18	29.20 (13)	—	—
S	—	1.517	1.515	1.525	1.527	1.515	1.529	1.527	1.531	1.537	1.523	1.525 (7)	—	—

isotropic/anisotropic R_{free} factor of 21.3/14.67 (Table 2, 'Overall' column). The average number of water molecules is 296 ± 6. These values can be compared with other published structures of native hen egg-white lysozyme: PDB entry 1dpx (Weiss *et al.*, 2000) with 177 water molecules and two chloride ions (resolution 1.65 Å, R = 18.7% and R_{free} = 24.6%), PDB entry 1iee (Sauter *et al.*, 2001) with 233 water molecules, one sodium and five chloride ions (resolution 0.94 Å, R = 12.3% and R_{free} = 15.1%), PDB entry 1jis (Datta *et al.*, 2001) with 141 water molecules (resolution 1.90 Å, R = 19.0% and R_{free} = 23.4%), PDB entry 1lz8 (Dauter *et al.*, 1999) with 224 water molecules, one sodium and eight chloride ions (resolution 1.53 Å, R = 22% and R_{free} = 31%) and PDB entry 1hel (Wilson *et al.*, 1992) with 319 water molecules (resolution 1.70 Å, R = 15.2%).

In total, 430 possible water-molecule positions were located within the final ensemble of ten models: 216 of these water molecules occurred in all ten models, 19 in nine models, 13 in eight models, 14 in seven models, 16 in six models, 16 in five models, 15 in four models, 21 in three models and 31 in two models; 69 water molecules are unique.

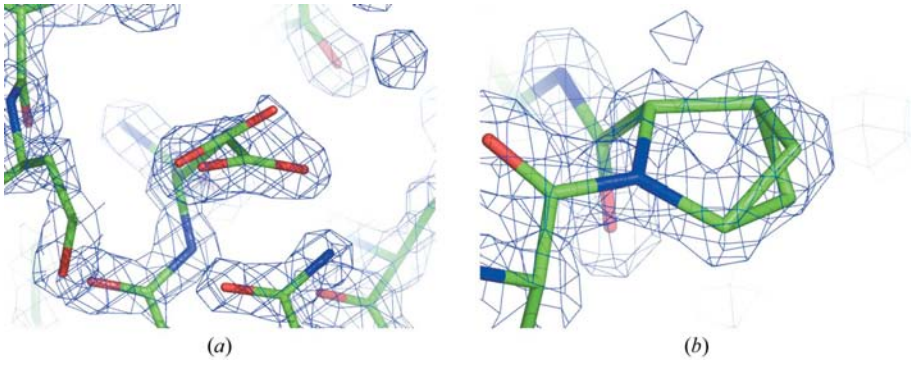

Figure 1
Modelled and refined disorder of (*a*) Asp52 and (*b*) Pro79. The electron-density map is contoured at 1.7σ (produced using *PyMOL*; DeLano, 2002).

3.2. Structures of bromates

For bromates *A* and *B* (model 1; occupancies 0.55 and 0.68, respectively), the positions of all the O atoms could be determined. O atoms O1_*A* and O3_*B* partially replace water molecules in the native structure and this slightly affects their calculated positions (partial occupancy) in the current structure (especially the water molecule at position

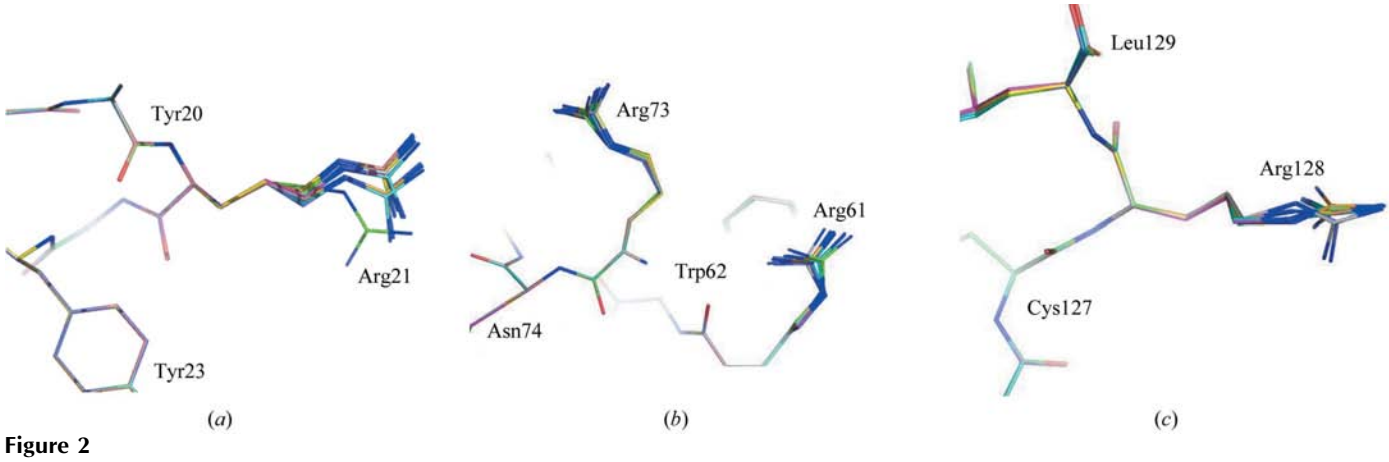

Figure 2
Examples of disorder generated by the refinement for (*a*) Arg21, (*b*) Arg61 and Arg73 and (*c*) Arg128 (produced using *PyMOL*; DeLano, 2002).

O1_*A*). Similar to the structure determined from inorganic bromate crystals, bromates *A* and *B* both form deformed octahedrons. Bromate *B* is probably present as an $HBrO_3$ species as the Br—O3 bond length is significantly longer than the other Br—O bonds, including those seen in inorganic bromate crystals. All other Br—O distances are about equal within the variance and are also shorter in comparison to those observed in inorganic crystals.

Bromates *A* and *B* form a dimer *via* their Br···O2 bonds: the calculated occupancies (0.55 and 0.68) argue for the existence of a bromate dimer with a Br_*A*···Br_*B* distance of 3.686 (5) Å. This dimer is approximately symmetrical through the symmetry centre. The structure is shown in Fig. 3 and further described in Table 3. Fig. 4 shows the positions of the bromates on the surface of a lysozyme molecule: the anomalous difference map further corroborates the existence of the dimer.

For each bromate, the three intermolecular Br···O interactions are roughly equal in length. For bromate *A*, they are somewhat shorter than those found in inorganic crystals. For bromate *B*, they are clearly shorter (up to ∼0.5 Å). A good explanation could be the presence of a hydroxyl group in bromate *B*. The presence of only one negative charge of the dimer is in good agreement with its position on the surface of the lysozyme molecule: there are no bonds to any charged group (arginine, histidine and aspartic or glutamic acid).

Oxygen O1_*A* is coordinated to water molecules W3 and either W4 or W5. The arrangement around the O1_*A* oxygen is in fact a superposition of the structure with and without bromate. Oxygen O2_*A* is coordinated to the backbone amides of Thr69 and Pro70 at a similar distance (see Table 3). Oxygen O3_*A* is hydrogen bonded to water molecules W3, W6 and either W7 or W8. Oxygen O1_*B* forms one hydrogen bond to water molecule W11 and is in contact with the backbone O atoms of Thr69 and Ser72. Oxygen O2_*B* forms a hydrogen bond to water molecules W9 and W10. Oxygen O3_*B* is most probably a hydroxyl group that forms two classical hydrogen bonds to the backbone amides of Gly67 and Arg68 and shares a proton with Thr69 N (the shortest distance out the three) that also can form a hydrogen bond to water W6. The angles O2_*A*—Br_*A*—O3_*A* and O1_*B*—Br_*B*—O2_*B*, which are not influenced by an overlap with a water molecule from the bromate-free structure (partial occupancy), are identical and significantly larger then those observed in inorganic crystals and are very close to the ideal value reported for a tetrahedron. The angles O1_*B*—Br_*B*—O3(H)_*B* and O2_*B*—Br_*B*—O3(H)_*B* are also identical but clearly smaller then those given for inorganic crystals. Finally, the angles O2_*A*—Br_*B*—O2_*B* and Br_*A*—O2_*B*—Br_*B* are practically regular.

A possible dimer is also observed for bromates *C* and *D* (occupancies 0.23 and 0.25), with a Br_*C*···Br_*D* distance of 3.74 (2) Å. The anomalous data allowed us to determine both the occupancy and position of these bromines but, owing to the low occupancy, we were not able to determine the oxygen positions adequately. One oxygen overlaps with a water molecule with a Br_*D*–O1_*D* distance of 1.73 (4) Å. This distance is very similar to that observed for the hydroxyl group in bromate *B* [1.717 (9) Å]. Br_*C* makes contacts to Lys33 O at 3.077 (14) Å and a water molecule (W12) at 2.75 (3) Å. O1_*D* makes contacts to Gly22 O at 2.923 (16) Å and to a symmetry-related Arg114 N (symmetry code $1/2 + y - 1$, $1/2 - x$, $1/4 + z$) at 2.99 (3) Å and its NE at 2.960 (15) Å.

Bromates *E*, *F*, *G*, *H* and *I* [occupancies 0.34 (2), 0.229 (12), 0.22 (2), 0.43 (4) and 0.20 (3), respectively] were determined as single ions on the basis of their anomalous signals. Their occupancies are too low and as a result the oxygen positions cannot be determined satisfactorily. Some of their O atoms replace water molecules in the structure and only a few deformed bond distances can be estimated.

Two O atoms of bromate *E* that overlap with water molecules have bond lengths of 1.75 (5) Å for Br_*E*–O1_*E* and 1.45 (4) Å for Br_*E*–O2_*E*. Oxygen O1_*E* is hydrogen bonded to Asn65 of a neighboring molecule (symmetry code *y*, *x*, $-z + 1$), with an O1_*E*···ND2 distance of 2.98 (4) Å, and one water molecule, with an O1_*E*···W13 distance of 2.55 (7) Å.

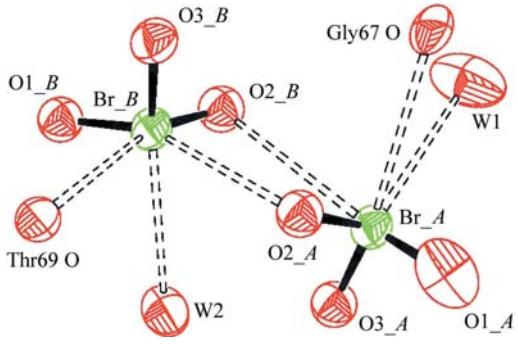

Figure 3
ORTEP-3 (Farrugia, 1997) presentation of $BrO_3^-\cdot HBrO_3$ dimer (*AB*).

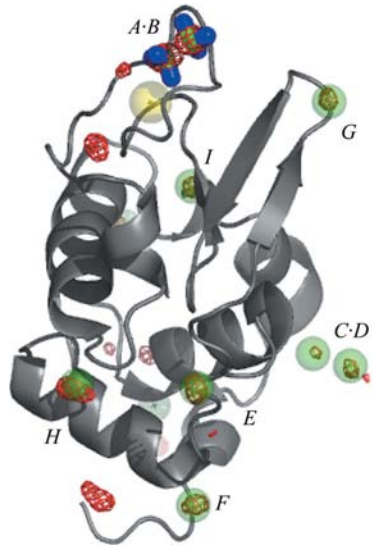

Figure 4
Lysozyme molecule showing bromates (green spheres, O atoms in blue), chlorines (lime spheres) and sodium (yellow sphere). The anomalous difference electron-density map (red) is contoured at 4σ; redundant maxima are from symmetry-related molecules (produced using *PyMOL*; DeLano, 2002).

Table 3
Selected interatomic and hydrogen-bond distances and angles of the $BrO_3^-HBrO_3$ dimer (*AB*).

Model	1	2	3	4	5	6	7	8	9	10	Mean (e.s.d.)
Distances (Å)											
Br_*A*—O1_*A*	1.50	1.54	1.43	1.54	1.52	1.51	1.46	1.42	1.47	1.40	1.48 (5)
Br_*A*—O2_*A*	1.58	1.60	1.60	1.64	1.62	1.59	1.59	1.59	1.56	1.60	1.60 (2)
Br_*A*—O3_*A*	1.61	1.59	1.61	1.59	1.58	1.56	1.57	1.58	1.56	1.56	1.58 (2)
Br_*A*···Gly67 O	3.15	3.16	3.16	3.17	3.18	3.16	3.16	3.16	3.16	3.14	3.161 (9)
Br_*A*···W1	3.21	3.16	3.17	3.17	3.17	3.18	3.22	3.20	3.17	3.21	3.19 (2)
Br_*A*···O2 _*B*	3.36	3.36	3.35	3.37	3.36	3.36	3.35	3.38	3.37	3.37	3.363 (9)
Br_*A*···Br_*B*	3.69	3.69	3.69	3.69	3.69	3.68	3.68	3.68	3.69	3.68	3.686 (5)
Br_*B*—O3_*B*	1.72	1.73	1.72	1.72	1.70	1.71	1.71	1.71	1.73	1.72	1.717 (9)
Br_*B*—O2_*B*	1.54	1.54	1.60	1.56	1.56	1.53	1.55	1.55	1.54	1.53	1.55 (2)
Br_*B*—O1_*B*	1.60	1.57	1.56	1.60	1.59	1.58	1.61	1.58	1.58	1.58	1.59 (2)
Br_*B*···O2_*A*	3.00	3.04	3.00	3.01	3.03	3.05	3.03	3.05	3.02	3.00	3.02 (2)
Br_*B*···Thr69 O	2.99	2.99	2.99	2.99	2.99	2.99	3.01	3.00	2.98	2.99	2.992 (7)
Br_*B*···W2	3.09	3.08	3.09	3.07	3.09	3.09	3.10	3.09	3.10	3.11	3.091 (10)
O1_*A*···W3	3.28	3.25	3.32	3.24	3.20	3.33	3.31	3.38	3.32	3.42	3.31 (6)
O1_*A*···W4	2.75	2.93	2.91	2.83	2.71	2.86	2.82	2.83	2.76	2.71	2.81 (7)
O1_*A*···W5	2.34	2.97	2.47	2.81	2.32	2.63	2.79	2.50	2.83	2.47	2.61 (21)
O2_*A*···Thr69 N	3.01	3.01	3.02	2.96	2.97	3.01	3.01	3.00	3.03	3.00	3.00 (2)
O2_*A*···Pro70 N	2.99	3.01	2.96	2.96	2.97	2.98	3.00	2.98	3.01	2.98	2.98 (2)
O3_*A*···W2	2.82	2.89	2.86	2.92	2.93	3.01	2.87	2.84	2.86	2.85	2.89 (5)
O3_*A*···W3	3.29	3.17	3.23	3.16	3.02	3.14	3.23	3.22	3.20	3.28	3.19 (7)
O3_*A*···W7	2.83	2.88	2.91	2.90	2.91	2.84	—	2.84	2.87	—	2.88 (3)
O3_*A*···W8	3.27	3.25	3.26	3.34	3.37	—	3.20	3.23	3.29	3.20	3.27 (5)
O3_*B*···Gly67 N	3.14	3.17	3.18	3.16	3.16	3.15	3.16	3.15	3.15	3.14	3.156(12)
O3_*B*···Arg68 N	3.14	3.13	3.13	3.12	3.13	3.17	3.14	3.15	3.14	3.14	3.139 (13)
O3_*B*···Thr69 N	2.95	2.93	2.93	2.93	2.94	2.99	2.95	2.96	2.95	2.94	2.947 (17)
O3_*B*···W6	2.72	2.73	2.70	2.72	2.73	2.72	2.72	2.72	2.71	2.72	2.719 (8)
O2_*B*···W9	2.73	2.71	2.79	2.77	2.77	2.80	2.86	2.72	2.66	2.71	2.75 (5)
O2_*B*···W10	2.91	2.79	2.85	2.96	2.81	2.84	2.80	2.91	2.83	2.90	2.86 (5)
O1_*B*···Thr69 O	3.24	3.20	3.19	3.19	3.20	3.20	3.22	3.19	3.20	3.22	3.205 (16)
O1_*B*···Ser72 OG	2.93	2.90	2.90	2.85	2.88	2.89	2.87	2.88	2.91	2.92	2.89 (2)
O1_*B*···W11	2.91	2.94	2.89	2.89	2.90	2.88	2.87	2.90	2.89	2.92	2.899 (19)
Angles (°)											
O1_*A*—Br_*A*—O2_*A*	102.18	101.13	101.93	100.51	101.63	99.70	99.77	99.99	100.85	100.46	100.8 (8)
O1_*A*—Br_*A*—O3_*A*	103.81	98.12	102.96	99.31	94.98	97.31	101.55	103.93	103.77	104.93	101 (3)
O2_*A*—Br_*A*—O3_*A*	108.97	109.06	107.34	107.40	107.22	109.49	109.53	109.04	108.08	108.80	108.5 (9)
O2_*A*—Br_*A*···O2_*B*	75.81	77.57	76.77	76.60	77.39	77.73	77.18	77.72	76.34	75.93	76.9 (7)
O2_*A*···Br_*B*—O2_*B*	88.83	89.54	88.81	90.16	89.66	89.37	89.08	89.92	88.70	89.46	89.4 (5)
Br_*A*···O2_*B*—Br_*B*	89.46	89.31	88.85	88.99	89.35	89.55	89.48	88.49	89.20	89.24	89.2 (3)
O2_*B*—Br_*B*—O3_*B*	101.97	102.73	101.85	102.15	102.76	101.67	102.93	102.04	102.24	101.76	102.2 (4)
O1_*B*—Br_*B*—O3_*B*	102.24	101.94	102.86	102.27	103.02	102.70	102.24	102.30	102.68	102.49	102.5 (3)
O1_*B*—Br_*B*—O2_*B*	107.33	108.18	109.19	109.13	108.70	108.95	109.27	108.85	108.27	108.11	108.5 (6)
O1_*A*—Br_*A*···O2_*B*	173.35	173.75	171.43	172.70	173.71	172.06	172.79	170.17	170.74	169.39	172.0 (14)
O1_B—Br_*B*···O2_*A*	159.56	158.35	157.13	156.73	157.22	156.87	157.20	157.12	158.53	158.41	157.7 (9)
Br_*B*—O3_*B*···W6	132.04	132.30	133.30	132.59	132.20	133.27	132.57	132.71	132.08	131.75	132.5 (5)

Oxygen O2_*E* is bound to Lys1 N, with an O2_*E*···Lys1 N distance of 3.21 (3) Å, and one water molecule, with an O2_*E*···W14 distance of 3.12 (5) Å. The presence of this bromate causes a disorder in the CG position of Pro79. This bromate is probably present as an $HBrO_3$ species.

Two O atoms of bromate *F* partly replace water molecules and have bond lengths of 1.615 (17) Å (for Br_*F*—O1_*F*) and 1.53 (3) Å (for Br_*F*—O2_*F*). The bromate O atoms are bound to Cys6 with O1_*F*···N = 2.99 (2) Å, water with O1_*F*···W15 = 3.27 (3) Å, Glu7 with O2_*F*···N = 2.957 (15) Å and another water molecule with O2_*F*···W16 = 3.18 (6) Å. A contact can be formed between bromine and a water molecule W17 at a distance of 2.90 (11) Å. This bromate probably exists as a BrO_3^- species.

The position of bromate *G* was only localized from a maximum in the difference anomalous map. The distance Br_*H*—O1_*H* of 1.73 (3) Å is indicative of the presence of a bromate *H*, resulting in an $HBrO_3$ species.

The distance Br_*I*—O1_*I* of 1.57 (3) Å is indicative of a BrO_3^- species. One oxygen can be bound to Asn59 N with an O1_*I*—N distance of 3.013 (14) Å.

4. Discussion

Because of uncertainties in the construction of the single structural model, we calculated an ensemble of ten models that enabled us to determine variances and statistically evaluate bond-length distances in the bromates. Each single model of the ensemble is equally compatible with the crystallographic data and as such the ensemble of models better describes the uncertainty of the experimental data and the structural micro-heterogeneity. The integrity of our approach was recently corroborated by Furnham *et al.* (2006).

All bromates located in the present structures were either one of two species, BrO_3^- or $HBrO_3$. Like periodate (Ondráček *et al.*, 2005), bromate seems to be able to accept or

release H^+ and thereby balance its charge depending on the chemical environment. Bromates *A* and *B* (and probably also bromates *C* and *D*) were found to form a dimer. In this dimer, one significantly longer Br—O bond could be modelled, clearly pointing to the presence of a $BrO_3^- \cdot HBrO_3$ dimer species. The observed O—Br—O angle is larger than those seen in inorganic crystals and it is practically identical with the ideal value for a tetrahedron.

For all bromate ions located within the tetragonal hen egg-white lysozyme crystal, the dominant bound positions were main-chain amide atoms. In contrast, periodate ions do not show such a clear preference for certain binding partners (Ondráček *et al.*, 2005). For the bromate dimer *AB*, five such bonds were found and for the rest of the bromates at least one such bond could be located. Between the nine bromates determined in the complex with lysozyme, only one (bromate *G*) was bonded to positively charged groups (Arg45 and Arg68). No bromate was found in the neighbourhood of a negatively charged group. An explanation for these observations cannot be exclusively found in the negative charge of the bromates themselves. In this case, one could expect the dominant bound position to be about an arginine and/or histidine. On the other hand, the negatively charged transition state of the substrate in many proteases is stabilized by the so-called oxyanion hole, which is often lined with backbone amide atoms. Because of the preferred binding to main-chain amide atoms (*i.e.* hardly any side chains are involved), bromates might prove more useful than other compounds in experimental phase determination.

The authors thank Rolf Hilgenfeld (Institute of Biochemistry, University of Lübeck) and Juraj Sedláček (Institute of Molecular Genetics, Academy of Sciences of the Czech Republic) for their generous support. This work was supported in part by project No. AV0Z50520514 awarded by the Academy of Sciences of the Czech Republic (ASCR) and the DAAD (ASCR D22-CZ28/04-05).

References

Abrahams, S. C. & Bernstein, J. L. (1977). *Acta Cryst.* B**33**, 3601–3604.
Collaborative Computational Project, Number 4 (1994). *Acta Cryst.* D**50**, 760–763.
Datta, S., Biswal, B. K. & Vijayan, M. (2001). *Acta Cryst.* D**57**, 1614–1620.
Dauter, Z. & Dauter, M. (1999). *J. Mol. Biol.* **289**, 93–101.
Dauter, Z. & Dauter, M. (2001). *Structure*, **9**, 21–26.
Dauter, Z., Dauter, M., de La Fortelle, E., Bricogne, G. & Sheldrick, G. M. (1999). *J. Mol. Biol.* **289**, 83–92.
Dauter, Z., Dauter, M. & Rajashankar, K. R. (2000). *Acta Cryst.* D**56**, 232–237.
Dauter, Z., Li, M. & Wlodawer, A. (2001). *Acta Cryst.* D**57**, 239–249.
DeLano, W. L. (2002). *The PyMOL Molecular Visualization System.* DeLano Scientific, San Carlos, CA, USA.
Farrugia, L. J. (1997). *J. Appl. Cryst.* **30**, 565.
Furnham, N., Blundell, T. L., DePristo, M. A. & Terwilliger, T. C. (2006). *Nature Struct. Mol. Biol.* **13**, 184–185.
Ondráček, J., Weiss, M. S., Brynda, J., Fiala, J., Jursík, F., Řezáčová, P., Jenner, L. B. & Sedláček, J. (2005). *Acta Cryst.* D**61**, 1181–1189.
Otwinowski, Z. & Minor, W. (1997). *Methods Enzymol.* **276**, 307–326.
Sauter, C., Otalora, F., Gavira, J.-A., Vidal, O., Giegé, R. & Garcia-Ruiz, J.-M. (2001). *Acta Cryst.* D**57**, 1119–1126.
Sheldrick, G. M. & Schneider, T. R. (1997). *Methods Enzymol.* **277**, 319–343.
Szafranski, M. & Stahl, K. (1994). *Z. Kristallogr.* **209**, 491–494.
Templeton, D. H. & Templeton, L. K. (1985). *Acta Cryst.* A**41**, 133–142.
Weiss, M. S., Palm, G. J. & Hilgenfeld, R. (2000). *Acta Cryst.* D**56**, 952–958.
Wilson, K. P., Malcolm, B. A. & Matthews, B. W. (1992). *J. Biol. Chem.* **267**, 10842–10849.